

File Copy

ESD RECORD COPY

RETURN TO
SCIENTIFIC & TECHNICAL INFORMATION DIVISION
(ESTI), BUILDING 1211

ESD ACCESSION LIST

ESTI Call No. 63111

Copy No. of cys.

Technical Note

1968-33

R. K. Crane

Simultaneous Radar
and Radiometer Measurements
of Rain Shower Structure

18 September 1968

Prepared under Electronic Systems Division Contract AF 19 (628)-5167 by

Lincoln Laboratory

MASSACHUSETTS INSTITUTE OF TECHNOLOGY

Lexington, Massachusetts



AD678079

The work reported in this document was performed at Lincoln Laboratory, a center for research operated by Massachusetts Institute of Technology, with the support of the U.S. Air Force under Contract AF 19(628)-5167.

This report may be reproduced to satisfy needs of U.S. Government agencies.

This document has been approved for public release and sale; its distribution is unlimited.

MASSACHUSETTS INSTITUTE OF TECHNOLOGY
LINCOLN LABORATORY

SIMULTANEOUS RADAR AND RADIOMETER MEASUREMENTS
OF RAIN SHOWER STRUCTURE

R. K. CRANE

Group 61

TECHNICAL NOTE 1968-33

18 SEPTEMBER 1968

LEXINGTON

MASSACHUSETTS

Simultaneous Radar and Radiometer Measurements of Rain Shower Structure

ABSTRACT

Simultaneous measurements of the backscatter cross section per unit volume and the sky temperature were made for limited volumes of rain showers using an L-band radar and an X-band radiometer. The object of the measurements was to provide data to validate the method used to compute attenuation and sky temperature given weather radar data as an input and to investigate the spatial changes in rainfall intensity and in the attenuation cross section per unit volume. The sky temperature was calculated using the radiative transfer equation and the distribution of attenuation cross section per unit volume estimated from the weather radar data. An empirical relationship between attenuation and backscatter cross sections was used based upon the results of a large number of Mie theory computations using measured rain-drop size distributions.

The results of the comparisons between calculated and measured sky temperature show good agreement. The discrepancies between the measured and calculated values are due to the difference in the antenna beamwidths for the two systems (0.6° for the L-band radar, 0.07° for the X-band radiometer). From these discrepancies the spatial distances over which the attenuation cross section can change significantly can be estimated. The results show that for the rain showers investigated, the attenuation cross section per unit

volume can change an order of magnitude in 400 meters and the integrated attenuation along a horizontal line-of-sight can change an order of magnitude for a 1.5 km horizontal translation of the path.

Accepted for the Air Force
Franklin C. Hudson
Chief, Lincoln Laboratory Office

Simultaneous Radar and Radiometer Measurements of Rain Shower Structure

I. INTRODUCTION

In the past few years considerable interest in the effects of rain on communication systems has been evidenced by the engineering community. The results of comparisons between estimated values of attenuation made from rain gauge data and simultaneously measured values of attenuation have shown poor agreement.¹⁻⁴ In several of the papers, the lack of agreement has been attributed to an inadequacy of scattering theory. It is the apparent lack of agreement between theory and measurement that lead to the present study.

The study consists of an analysis of a series of simultaneous high resolution L-band radar and X-band radiometer measurements of isolated rain showers. From these measurements the adequacy of scattering theory can be inferred and the problems of making detailed weather radar measurements for use in estimating attenuation can be defined. The radar system used for the measurement program has a 0.6-degree beamwidth and a 10-microsecond pulse length yielding an effective resolution volume of 1.44 cubic kilometers at a range of 100 kilometers. The radiometer system had a beamwidth of 0.07 degrees and an output dependent upon a weighted integral of the attenuation along the path in accordance with radiative transfer theory. The measurements from both systems were compared after the appropriate range integral of the radar data was computed.

The results of the comparisons of the radiometric and integrated radar data show no obvious discrepancies in scattering theory. The results do show that fluctuations in rain intensity occur at small scale sizes with scales smaller than that resolvable with the radar.

II. RADAR MEASUREMENTS

The radar system used for the measurements was the Millstone Hill Radar as described in Table I. The receiver system was calibrated each time an average value was prepared using a calibrated noise source. The radar receiver and recording system had an overall dynamic range of 50 db with an RMS error in cross section determination of less than 0.6 db. The constants in the point target radar equation were measured and confirmed with measurements on satellites with known cross sections. The distributed target radar equation was generated using the measured antenna pattern and receiver response curve. For a uniformly distributed target, the overall uncertainty in the calibration constants is less than 1.0 db. The minimum detectable target with this system is 24 db below a value of $Z = 1 \text{ mm}^6/\text{m}^3$ for a 10 db target to noise ratio at a range of 100 km. For rain observations, 40 to 60 db of attenuation was inserted between the antenna and receiver.

Two major problems exist in using a radar for attenuation estimation, the determination of the backscatter cross section per unit volume from which Z is calculated and the estimation of the attenuation cross section per unit volume using Z . The determination of Z given the measured backscatter cross

section was considered.⁵ For a matched filter receiver, the problem is slightly different due to the integrating action of the filter. Starting with the basic radar equation for a distributed target

$$P_{\text{rec}}(r, \alpha, \epsilon) = \frac{G_o^2 \lambda^2 P_{\text{trans}}^{\ell}}{(4\pi)^3} \int_0^{\infty} \int_0^{2\pi} \int_{-\pi}^{\pi} g^2(\alpha, \alpha', \epsilon, \epsilon') \beta(r', \alpha', \epsilon') \cdot h(r - r') \cos \epsilon' d\epsilon' d\alpha' \frac{dr'}{r'^2} \quad (1)$$

where $g(\alpha, \alpha', \epsilon, \epsilon')$ is the one-way antenna directivity pattern,
 $h(r - r')$ is the point target response function of the receiver system,
 $\beta(r', \alpha', \epsilon')$ is the backscatter cross section per unit volume as distributed in space,
 λ = wavelength, ℓ = line loss, G_o = antenna gain,
 P_{trans} = peak transmitter power,
 P_{rec} = received power, and
 r', α', ϵ' are range, azimuth and elevation coordinates, respectively.

For the Millstone Radar, the g and h functions were empirically determined. The integral is separable in range and angle coordinates if β is uniform over all space. Under these conditions the radar equation is given by

$$P_{\text{rec}}(r) = \frac{G_o^2 \lambda^2 P_{\text{trans}}^2}{(4\pi)^3 r^4} \sigma$$

$$\sigma = r^2 F \rho \beta \quad (2)$$

where

$$F = \int_0^{2\pi} \int_{-\pi}^{\pi} g^2(\alpha, \alpha', \epsilon, \epsilon') \cos \epsilon' d\epsilon' d\alpha' = 9.43 \times 10^{-5} = 0.855 \vartheta_{\text{hp}}^2$$

ϑ_{hp} = half-power beamwidth

$$\rho = r^2 \int_0^{\infty} \frac{h(r-r') dr'}{r'^2} = 1.53 \text{ km} = 1.02 \left(\frac{\tau c}{2}\right)$$

τ = pulse length, c = velocity of light.

For this radar, the response to a target of range extent less than or equal to ρ , is spread over two or three range boxes and is reported accurately only when these contributions are summed. Z is obtained from β by

$$Z = \frac{\lambda^4 \beta \times 10^{18}}{\pi^5 \frac{\epsilon - 1}{\epsilon + 2}} \quad (\text{mm}^6 / \text{m}^3) \quad (3)$$

where β = backscatter cross section per unit volume (m^2 / m^3)

ϵ = complex dielectric constant of water

λ = wavelength (m).

The attenuation cross section per unit volume can be estimated from Z only when the scattering properties of the meteorological elements are known. For rain, it is postulated that the drops are spherical, at a uniform temperature, and contribute singly to the formation of the scattered field. With these assumptions, Mie theory can be used to compute both Z and the attenuation coefficient per unit volume for any distribution of rain-drop sizes. For wavelengths longer than 3 cm the above assumptions appear to be valid and only the drop-size distribution is uncertain. Computations were made using the Illinois State Water Survey drop-size data⁶⁻⁹ to determine the drop-size distributions. Simple regression analysis was used to establish a relationship between the attenuation coefficient and Z for drop-size data from several locations as shown in Table II. The root mean square deviation of the errors in estimating the attenuation coefficient given Z are also given and serve to establish the uncertainty present in using the regression model. For comparison, a similar analysis for the attenuation coefficient as a function of rain rate is also included.

The radar data was converted into an attenuation estimate using the regression coefficients for the Miami data. This data was selected because of its showery nature and because the difference in the attenuation estimate for attenuations greater than .01 db/km made using any pair of regression coefficients is not significant. The attenuation measurements and estimates may be different because of the statistical variation in the Z , attenuation

coefficient relationship and because of the size of the storm volumes that contribute most to radar return. If the storm volume or cell that contributes most to the radar return is smaller than or equal to the size of the resolution volume, the attenuation will be overestimated. Figure 1 shows the percent error in estimating attenuation for an idealized situation where the cell has one Z value and the surrounding area has a much lower Z value. The error was computed by using a model storm for which the attenuation and Z value is known and performing the convolution operation indicated in Eq. (1) to obtain first the radar estimate of Z, then the attenuation estimate using the attenuation coefficient, Z relationship for each range resolution cell and finally summing over the extent of the model cell. The data on Fig. 1 also shows the error in estimating rain rate for a cell size smaller than the resolution volume for the standard $Z = 200R^{1.6}$ relationship. For radars with larger resolution volumes, the errors are larger.

The brightness temperature was computed from the radar estimates of attenuation coefficient for each resolution box using a simplified radiative transfer equation. In the X-band region the single scattering albedo or the ratio of the total scattering cross section to the extinction cross section is less than $.1^{10}$ and a single scattering approximation to the radiative transfer equation may be used.

For a rain-filled atmosphere with no sources beyond, the simplified radiative transfer equation is

$$T_B = \int_0^{\infty} \left[\frac{a(r)}{4.34} \right] T(r) e^{-\int_0^r \frac{a(r) dr}{4.34}} dr \quad (4)$$

where $a(r)$ is the attenuation coefficient in db/unit length, and

$T(r)$ is the drop temperature in °K.

T_B is the brightness temperature in °K.

The brightness temperature was computed for $T(r) = 273^\circ\text{K}$ and assumed constant over all space and time. This differs slightly from reality, but at the distances and heights in the atmosphere at which measurements were made, the resultant value of brightness temperature is in error by less than three percent. For comparison with the radiometer measurements, the brightness temperature is further corrected for the effects of the antenna and radome of the radiometer system. Error limits were also computed for the composite root mean square uncertainty in the attenuation coefficient due to the uncertainty in the radar cross section measurements and the attenuation coefficient, Z , relationship

$$\frac{ae}{a_{\text{rms}}} = 1 + \sqrt{(\gamma - 1)^2 + (\beta 0.14)^2} \quad (5)$$

When the β and γ coefficients from Table II are used, $ae/a = 1.35$ for the root mean square attenuation estimates error. A second set of error limits

were also computed to show the effort of a cell of 400 m size. A typical estimation of attenuation as a function of azimuth relative to the radar is given in Fig. 2. The points are the actual estimates and the error limits are due both to the statistical measurement uncertainty and the composite effect of statistical measurement uncertainty and small scale-size rain cell.

The attenuation estimates and brightness temperature estimates are valid only for liquid water targets. If hail is present in the scattering volume, the attenuation will be overestimated by an unknown amount. If snow is present, the results will also be in error. For purposes of comparison, only isolated summer rain showers were used with peak estimated rain intensities less than 150 mm/hr. This was done in an attempt to insure observation only of liquid rain.

III. RADIOMETER MEASUREMENTS

The radiometer system used for the measurement program was a part of the Haystack Microwave Research Facility and is described in Table III. The radiometer system was used to scan the rain showers at low elevation angles. At the low elevation angles a considerable fraction of the power detected comes from the ground through the antenna side lobes. The system was used to measure the relative change in antenna temperature as a function of antenna pointing angles. On clear days, azimuth scans were made at fixed elevation angles to determine the uncertainty in temperature determination due to variations in the ground, side-lobe energy contribution to the antenna tempera-

ture. For the range in elevation and azimuth angles used, the uncertainty was less than 4°K peak to peak.

The antenna efficiency for the antenna and radome system was evaluated using a series of elevation scans on clear days. The expected variation of atmospheric brightness temperature determined from rawinsonde soundings was compared with the measured antenna temperature. The differences were used to model the main lobe and side-lobe response of the antenna system at low elevation angles. The relationship determined was

$$T_A = \left[0.79 T_B + 0.21 T_{S(\epsilon)} \right] e^{- (1.2/4.34)} = .60 T_B + .16 T_{S(\epsilon)} \quad (6)$$

where

T_A = antenna or measured temperature.

T_B = atmospheric brightness temperature.

$T_{S(\epsilon)}$ = elevation angle dependent side-lobe temperature and the radome provides 1.2 db attenuation.

The coefficients in the equation were elevation angle dependent, but over the range of elevation angles used, 1.° to 3.°, the dependence may be neglected.

The radiometer system measures a weighted integral of attenuation along a narrow cone of rays passing through the atmosphere as described by Eq. (4), when the side-lobe contributions are assumed constant and the single scattering albedo is small. At X-band the conditions on Eq. (4) are met for atmospheric

gases, clouds, and rain. A radiometric measurement detects the presence of all these.

$$T_B = \int \frac{(a_{\text{gas}} + a_{\text{cloud}} + a_{\text{rain}})}{4.34} T e^{-\left\{ \int a_{\text{gas}} + a_{\text{cloud}} + a_{\text{rain}} \frac{dr}{4.34} \right\}} dr .$$

In the simplest case where a and T are independent of r

$$T_B = T \left[1 - e^{-\frac{(a_{\text{gas}} + a_{\text{cloud}} + a_{\text{rain}}) R}{4.34}} \right] .$$

For typical atmospheric conditions and at a $2.^\circ$ elevation angle, the total attenuation due to atmospheric gases is of the order of 1 db and is essentially constant as a function of azimuth. The variable contributions for an azimuth scan are caused by clouds and rain. The cloud contribution is related to the liquid water content of the cloud integrated along the path as given by Rayleigh¹¹ theory.

$$a_{\text{cloud}} = 0.05 L \text{ (db/km)}$$

where $L = \text{liquid water content in gm/m}^3$.

For 10 km of 1 gr/m^3 liquid water content in clouds, the total attenuation is 0.5 db resulting in a brightness temperature of 30°K . This value is about the peak cloud attenuation observed during the measurement period. For the occurrence of both clouds and rain, the attenuations add and the error caused

in estimating attenuation is less than 10 percent for rain attenuation in the 5 to 10 db range for the above value of cloud attenuation.

IV. COMPARISON OF MEASUREMENTS

Data was taken for the purpose of comparing radar and radiometer measurements on two days during July 1967. About two hours of useful data resulted on isolated shower systems of less than 40 km in horizontal extent located 80 to 160 km from the radar station. The observations were made by scanning the radar and radiometer in azimuth through the directions to the showers. Both antenna systems were computer directed to simultaneously observe at the same azimuth and elevation. For the comparison of results the azimuth from the radar was corrected for parallax error (the distance between the antennas was 0.688 km) and is reported as azimuth from the radiometer. Both systems did not observe the same storm volumes simultaneous but the smaller volume looked at by the radiometer was within that looked at by the radar. The scan rate was adjusted so that both antennas moved approximately half a beamwidth per integration interval.

Typical data for an azimuth scan is given in Fig. 3 where the temperature scale is temperature relative to a clear sky at 2° elevation angle. The radar generated temperature estimates are given by the dots with the rms error estimates given as the dotted lines. The small crosses represent the radiometer measurements. Because the radiometer beamwidth is about one-tenth that of the radar, a direct comparison of measurements is difficult to analyze.

For comparison, the radiometer data was averaged over the azimuthal extent of the radar beamwidth and is reported as a circle on the figure. The data was averaged uniformly over the interval. A weighted averaging using the antenna patterns should be used, but was not in this study.

The final comparison is given in Fig. 4 where the azimuth averaged temperature measurements are plotted vs. the radar estimates. The expected maximum measured temperature relative to the clear sky temperature at a 2° elevation angle for a black body at 273°K was 130°K using an estimated 1 db attenuation due to atmospheric gases between the storm and the radiometer. The peak measured temperature of 140°K is in excess of that possible due to thermal radiation. This could signify that some of the radiation from the storm is non-thermal as proposed by Sartor and Atkinson,¹² that the 2° reference temperature was in error by 10°K or that the attenuation due to atmospheric gases between the storm and the radiometer was 0.68 db rather than 1. as assumed. The curved lines show the expected rms variation, the expected rms variation corrected for a limited target, 400 m in extent and the maximum variation for the drop distribution samples used to generate Table II. Except for the low values of estimated temperature and the measured values above 130°K agreement between the measured and estimated temperatures is evident. The lack of agreement between the low estimated temperature values and the measured values is due to clouds.

The comparison for both days of measurements are given in Figs. 5 and

6. The comparison data has the same general feature as shown by the single azimuth scan data. In addition, these figures show some data points representing measured attenuations lower than expected due to variations of the drop-size distributions. A closer analysis of the data indicates that these points are caused by the antenna beamwidth size differences which are not exactly accounted for by the method of azimuth averaging used above.

An analysis of Figs. 2 and 3 shows that the regions of the rain showers contributing to the attenuation are very small. The radar data show attenuation peaks of 10 db occurring over azimuth intervals of 1. - 2. ° or 2 - 4 km horizontal extent. The change from 2 to 10 db can occur over angles less than a half degree or for horizontal motion of the path by less than 1.2 km. The radiometer data of Fig. 3 shows even finer scale changes in the rain structure. At the peak temperature values, variations of a few db over angular distances of tenths of degrees are evident. This translates into a few db change in less than 300 to 400-meter horizontal translation of the path. The radar PPI plot for this azimuth scan is given in Fig. 7. The small scales of rain structure are evident here and are consistent with the radiometer estimate that significant changes in storm structure occur over 400-m distances.

V. CONCLUSIONS

The comparison between radiometric measurements and radar estimates of rain brightness temperature show that the estimates and measurements are in agreement within the uncertainty present in the variability of drop-size

distributions. This shows that at a frequency where multiple scattering is not an important consideration, agreement is obtained with scattering theory and that high resolution radars can provide meaningful estimates of attenuation. The question still remains as to why previously reported attenuation measurements do not agree well with estimates made using rain-rate measurements. The answer apparently is in the inadequacy of point rain-rate measurements for use in the estimation of attenuation along a path. For showery rain with significant changes in rain intensity over spatial distances of 400 meters, a network of widely spaced gauges is inadequate to describe the instantaneous attenuation along a path.

TABLE I

Radar Parameters

| | |
|-------------------------------------|---|
| Frequency | 1.295 GHz (23.2 cm wavelength). |
| Antenna | 84-foot parabola with Cassegrain feed. |
| Antenna gain | 47.1 db. |
| Polarization | Right-hand circular transmitted left-hand circular received. |
| Beamwidth | 0.6° between half-power points. |
| Transmitted power | 1.25 Mw peak (continuously monitored). |
| Pulse length | 10 μsec. |
| Pulse repetition rate | 20 per second. |
| Receiver bandwidth | 10 μsec matched predetection filter. |
| Data processing | Analog and digital converter operating at 10 μsec sampling rate. |
| Detection | Square law by computer operations. |
| Post detection filter | 50 pulse average. |
| System noise temperature | 190°K. |
| Overall system feed and line losses | 1.7 db. |

TABLE II

Regression Coefficients for Computations of Attenuation

$f = 7.78 \text{ GHz } (\lambda = 3.86 \text{ cm})$

$T = 0^\circ\text{C}$

No.

| Location | A vs. Z [†] | | | | A vs. R [†] | | | |
|----------------------------|-----------------------|---------|----------|----------|-----------------------|---------|----------|------|
| | α | β | γ | δ | α | β | γ | |
| Miami (8 GHz) [‡] | 4.39×10^{-5} | 0.852 | 1.26 | - | - | - | - | 2483 |
| Illinois '53 - '63 | 5.16×10^{-5} | 0.814 | 1.29 | 1.33 | 6.62×10^{-3} | 1.14 | 1.34 | 1532 |
| Illinois '64 | 3.69×10^{-5} | 0.851 | 1.22 | 1.26 | 6.12×10^{-3} | 1.18 | 1.28 | 185 |
| Miami | 3.58×10^{-5} | 0.864 | 1.23 | 1.26 | 6.03×10^{-3} | 1.13 | 1.32 | 2506 |
| Oregon | 8.31×10^{-5} | 0.744 | 1.25 | 1.31 | 6.20×10^{-3} | 1.12 | 1.23 | 1703 |
| Marshall Islands | 7.32×10^{-5} | 0.808 | 1.38 | 1.47 | 5.98×10^{-3} | 1.03 | 1.15 | 1314 |
| All Data | - | - | - | 1.33 | - | - | - | 7240 |

$$\dagger A_e = \alpha x^\beta$$

where A_e = attenuation coefficient = db/km.

α, β are regression coefficients.

$x = Z$ or R in mm^6/m^3 or mm/hr .

$\gamma = 10 \left\{ \frac{1}{N} \sum (\log A - \log A_c)^2 \right\}$ rms difference between estimated attenuation and computed attenuation.

$\delta = 10 \left\{ \frac{1}{N} \sum (\log A - A_m)^2 \right\}$ rms difference between model attenuation and computed attenuation.

N = The number of drop-size distributions used in the regression analysis.

[‡] The location refers to Illinois State Water Survey data used for the attenuation computations. The Miami (8 GHz) refers to the model which was computed for a 8.0 GHz frequency not 7.78 as used for the measurements.

TABLE III

Radiometer Parameters

| | |
|--|---|
| Frequency | 7.78 GHz (3.86 cm). |
| Antenna | 120-foot parabola with Cassegrain feed. |
| Polarization | Left-hand circular. |
| Beamwidth | 0.07° between half-power points. |
| Receiver Bandwidth | 16 MHz predetection. |
| Detector | Switched comparison-type radiometer. |
| Integration Period | 0.3 seconds. |
| System Noise Temperature | 60° K. |
| Temperature Measurement Uncertainty | 0.03° K. |

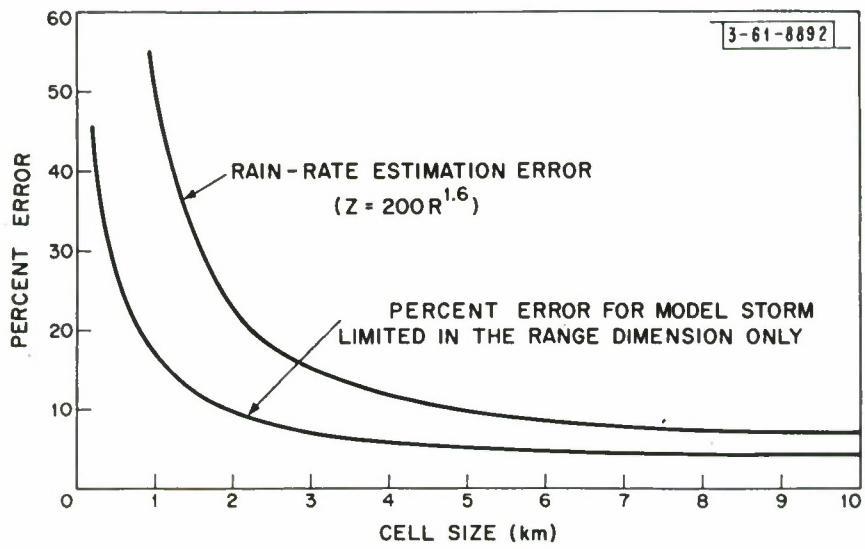
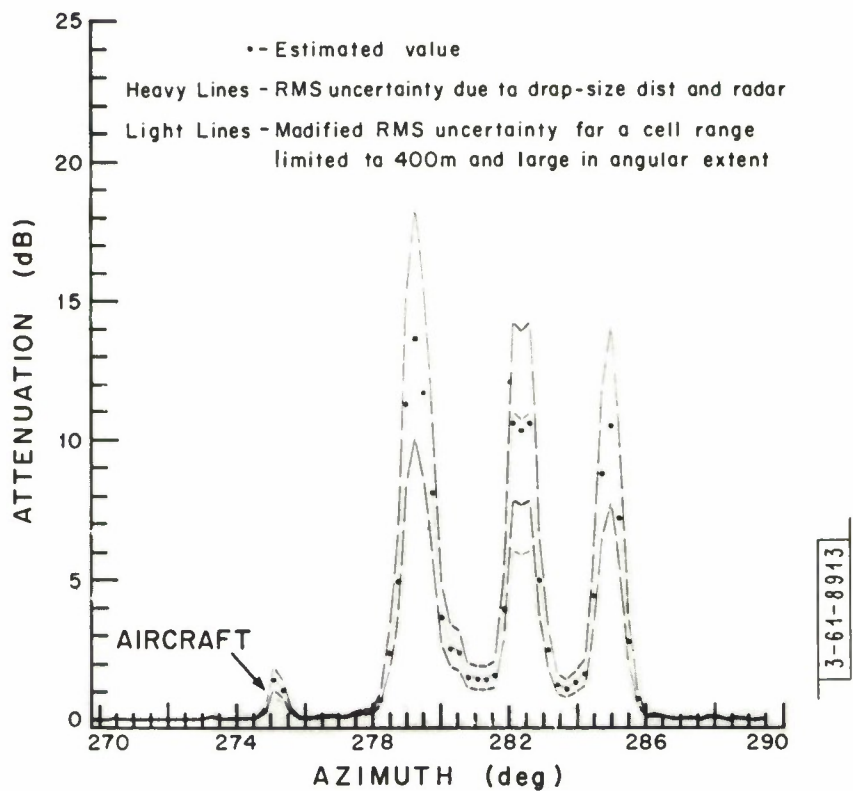


Fig. 1. Percent measured error vs. cell size.



24 JUL 1967 2052 GMT 1.4 - DEG ELEVATION

Fig. 2. Estimated attenuation using Millstone Hill Radar data.

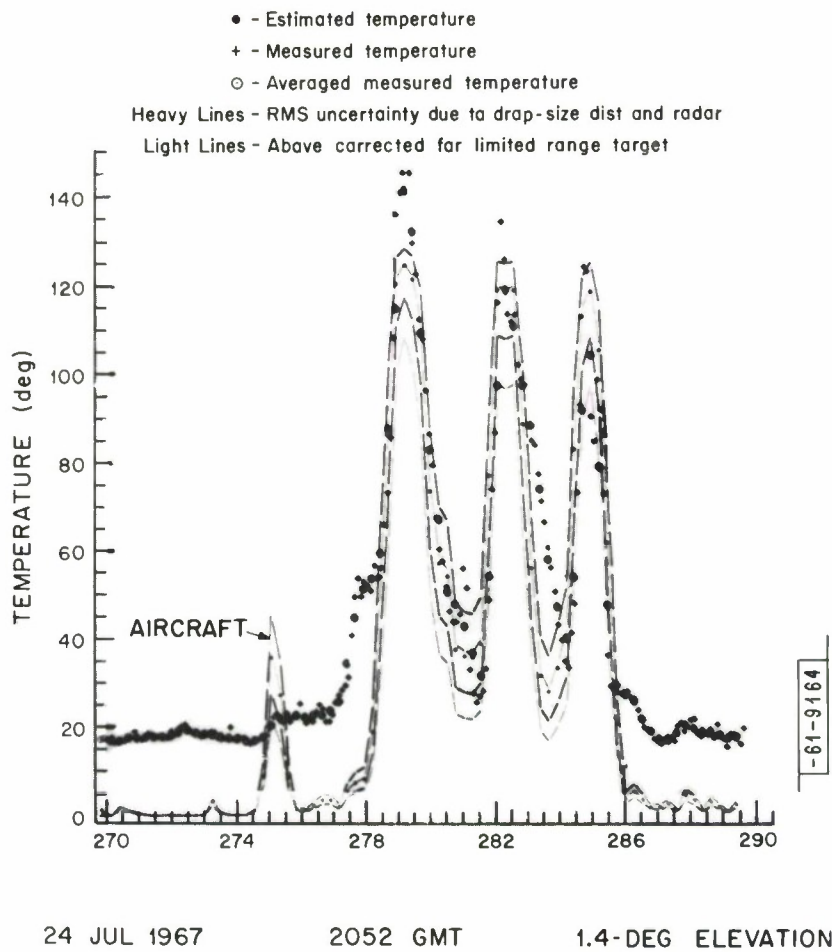
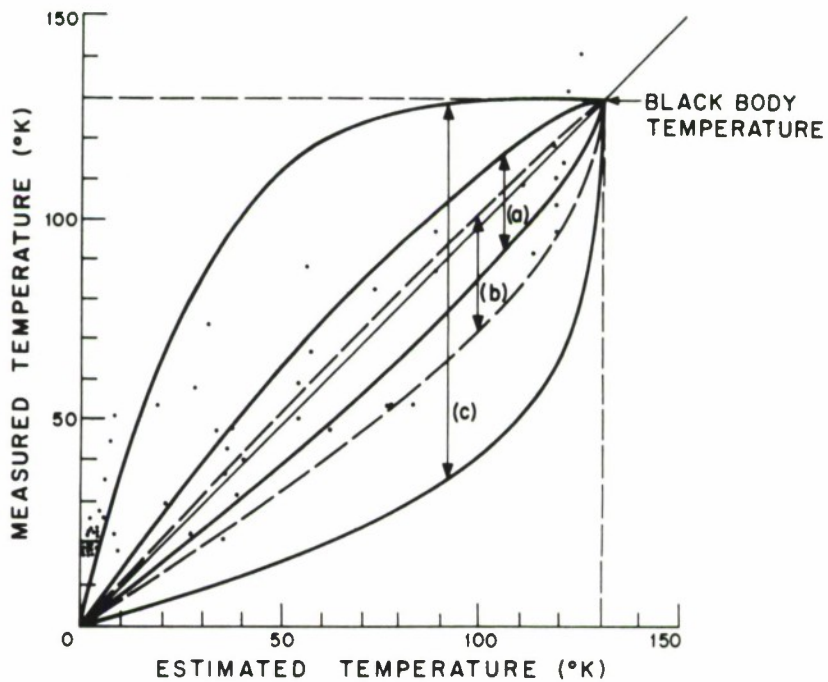


Fig. 3. Estimated and measured temperature relative to a 2-degree clear sky value using Millstone Hill Radar data.

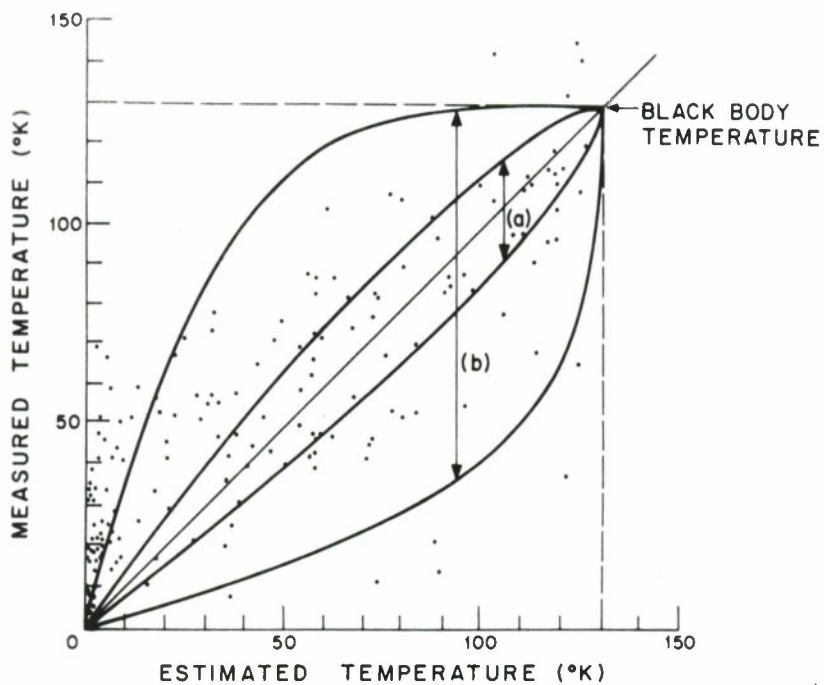


- (a) Measured values within RMS uncertainty due to drop-size distribution and radar
- (b) Same as above except corrected for a distributed target of 400-m extent in range
- (c) Measured data within peak uncertainty due to drop-size distribution

-61-9165

24 JUL 1967 2052 GMT 1.4° ELEVATION 270-290° AZIMUTH

Fig. 4. Comparison between Millstone Hill Radar and Haystack radiometer data - one scan.



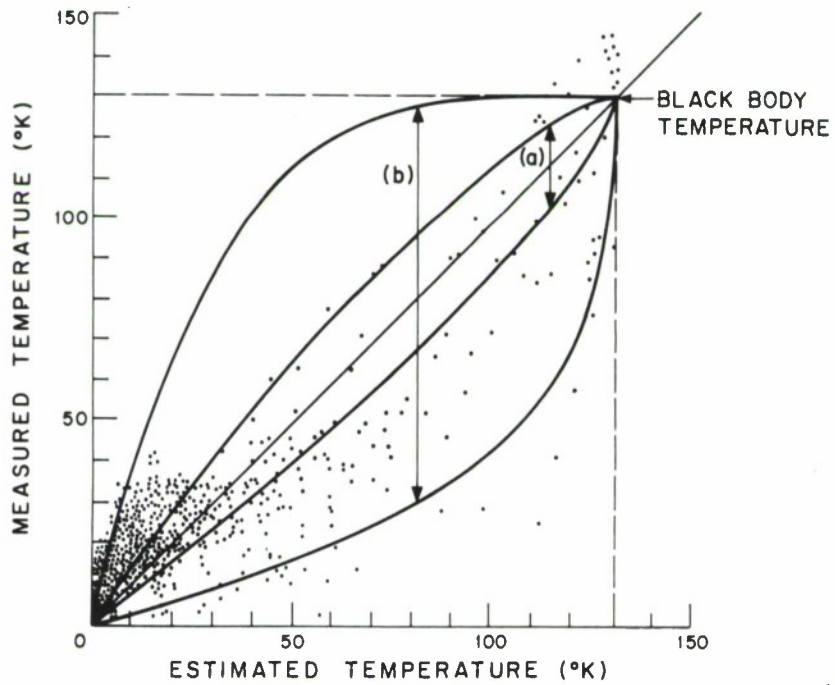
- (a) Measured values within RMS uncertainty of estimate due to drop-size distribution and radar
- (b) Measured values within peak uncertainty of estimate due to drop-size distribution

- 61 - 9166

24 JUL 1967

1 to 2° ELEVATION ANGLES

Fig. 5. Comparison between Millstone Hill Radar and Haystack radiometer data.



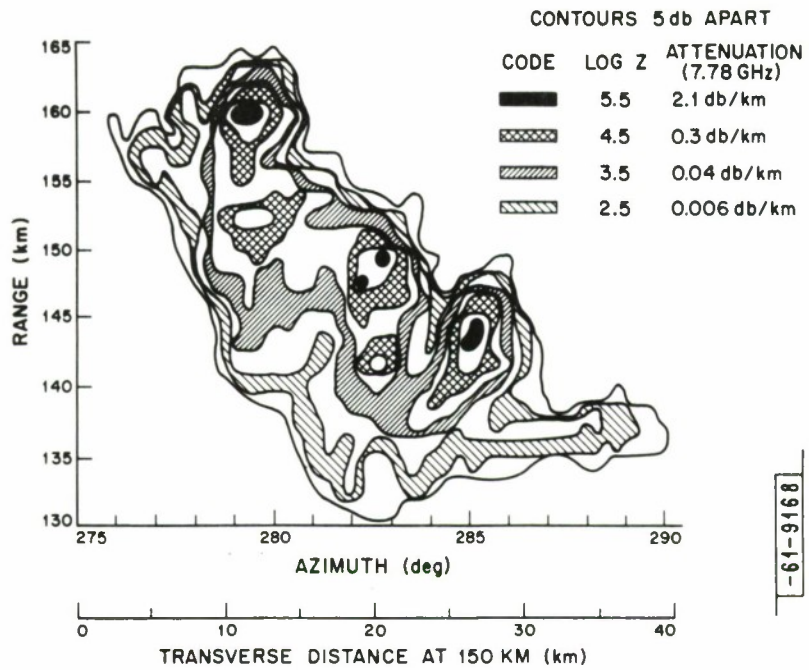
- (a) Measured dots within RMS uncertainty due to drop-size distribution and radar
- (b) Measured dots within peak uncertainty due to drop-size distribution

-61-9167

31 JUL 1967

1 to 2° ELEVATION ANGLES

Fig. 6. Comparison between Millstone Hill Radar and Haystack radiometer data.



WEATHER RADAR DATA
24 JUL 1967 2052 GMT

MILLSTONE HILL RADAR
1.4° EL, 275°-290° AZ

Fig. 7. Contour map of rain intensity.

REFERENCES

1. R. G. Medhurst, "Rainfall Attenuation of Centimeter Waves: Comparison of Theory and Measurement," *IEEE Trans. Antennas Propag.* AP-13, No. 4, 550-564 (1965).
2. J. Bell, "Propagation Measurements at 3.6 and 11 Gc/s over a Line-of-Sight Path," *Proc. IEE* 114, No. 5, 545-549 (1967).
3. B. J. Easterbrook, "Prediction of Attenuation by Rainfall in the 10.7 - 11.7 GHz Communication Band," *Proc. IEE* 114, No. 5, 557-565 (1967).
4. B. C. Blevis, R. M. Dohoo and K. S. McCormick, "Measurements of Rainfall Attenuation at 8 and 15 GHz," *IEEE Trans. Antennas Propag.* AP-15, No. 3, 394-403 (1967).
5. J. R. Probert-Jones, "The Radar Equation in Meteorology," *Quart. J. Roy. Meteorol. Soc.* 88, 485-495 (1962).
6. E. A. Mueller, "Raindrop Distributions at Miami, Florida," Research Report No. 9B, Illinois State Water Survey Meteorological Laboratory, Urbana, Illinois (1962).
7. E. A. Mueller, data for Illinois, (private communication).
8. E. A. Mueller and A. L. Sims, "Raindrop Distributions at Covallis, Oregon," Res. and Dev. Tech. Report ECOM-02071-RR6, Atmosphere Sciences Laboratory, U.S.A. Electronics Command, Ft. Monmouth, N. J. (1968).
9. E. A. Mueller and A. L. Sims, "Raindrop Distributions at Majuro Atoll, Marshall Islands," Res. and Deve. Tech. Report ECOM-02071-RR1, Atmospheric Sciences Laboratory, U.S.A. Electronics Command, Ft. Monmouth, N. J. (1967).
10. R. K. Crane, "Microwave Scattering Parameters for New England Rain," Technical Report 426, Lincoln Laboratory, M.I.T. (1966), AD 647798.
11. K. L. S. Gunn and T. W. R. East, "The Microwave Properties of Precipitation Particles," *Quart. J. Roy. Meteorol. Soc.*, 80, 522-545 (1954).
12. J. D. Sartor and W. R. Atkinson, "Charge Transfer Between Raindrops," *Science*, 157, No. (3795), 1267-1269 (1967).

| DOCUMENT CONTROL DATA - R&D | | |
|---|--|-----------------------|
| <i>(Security classification of title, body of abstract and indexing annotation must be entered when the overall report is classified)</i> | | |
| 1. ORIGINATING ACTIVITY (Corporate author) Lincoln Laboratory, M.I.T. | 2a. REPORT SECURITY CLASSIFICATION Unclassified | |
| | 2b. GROUP None | |
| 3. REPORT TITLE Simultaneous Radar and Radiometer Measurements of Rain Shower Structure | | |
| 4. DESCRIPTIVE NOTES (Type of report and inclusive dates) Technical Note | | |
| 5. AUTHOR(S) (Last name, first name, initial) Crane, Robert K. | | |
| 6. REPORT DATE 18 September 1968 | 7a. TOTAL NO. OF PAGES 30 | 7b. NO. OF REFS 12 |
| 8a. CONTRACT OR GRANT NO. AF 19(628)-5167 | 9a. ORIGINATOR'S REPORT NUMBER(S) Technical Note 1968-33 | |
| b. PROJECT NO. 649L | 9b. OTHER REPORT NO(S) (Any other numbers that may be assigned this report) ESD-TR-68-266 | |
| c. | | |
| d. | | |
| 10. AVAILABILITY/LIMITATION NOTICES This document has been approved for public release and sale; its distribution is unlimited. | | |
| 11. SUPPLEMENTARY NOTES None | 12. SPONSORING MILITARY ACTIVITY Air Force Systems Command, USAF | |
| 13. ABSTRACT Simultaneous measurements of the backscatter cross section per unit volume and the sky temperature were made for limited volumes of rain showers using an L-band radar and an X-band radiometer. The object of the measurements was to provide data to validate the method used to compute attenuation and sky temperature given weather radar data as an input and to investigate the spatial changes in rainfall intensity and in the attenuation cross section per unit volume. The sky temperature was calculated using the radiative transfer equation and the distribution of attenuation cross section per unit volume estimated from the weather radar data. An empirical relationship between attenuation and backscatter cross sections was used based upon the results of a large number of Mie theory computations using measured raindrop size distributions. The results of the comparisons between calculated and measured sky temperature show good agreement. The discrepancies between the measured and calculated values are due to the difference in the antenna beamwidths for the two systems (0.6° for the L-band radar, 0.07° for the X-band radiometer). From these discrepancies the spatial distances over which the attenuation cross section can change significantly can be estimated. The results show that for the rain showers investigated, the attenuation cross section per unit volume can change an order of magnitude in 400 meters and the integrated attenuation along a horizontal line-of-sight can change an order of magnitude for a 1.5 km horizontal translation of the path. | | |
| 14. KEY WORDS radar cross sections radiometry L-band radars X-band radiometers | | |